

Published in Journal of Vascular Surgery.

Full reference: Zilla P, Moodley L, Wolf MF, Bezuidenhout D, Sirry MS, Rafiee R, Lichtenberg W, Black M, Franz T. Knitted nitinol represents a new generation of constrictive external veingraft meshes. J Vasc Surg, 2011, 1
DOI: 10.1016/j.jvs.2011.05.023

KNITTED NITINOL REPRESENTS A NEW GENERATION OF CONSTRICTIVE EXTERNAL VEINGRAFT MESHES

Peter Zilla⁺, Loven Moodley⁺, Michael F. Wolf^{*}, Deon Bezuidenhout⁺, Mazin S. Sirry⁺, Nasser Rafiee[#], Wilhelm Lichtenberg⁺, Melanie Black⁺ and Thomas Franz⁺

+ Christiaan Barnard Department of Cardiothoracic Surgery, University of Cape Town, South Africa

* Medtronic Science and Technology, Medtronic Inc., Minneapolis, MN

Competition of interests: The study was supported by a grant from Medtronic. Deon Bezuidenhout, Nasser Rafiee, Michael Wolf, Thomas Franz and Peter Zilla are inventors on patents on the technology described in the study. At the time of the study, Nasser Rafiee reported consulting fees from Medtronic and Michael Wolf was an employee of Medtronic.

Send correspondence to:

Peter Zilla, MD, PhD

Chris Barnard Division of Cardiothoracic Surgery

University of Cape Town

Faculty of Health Sciences

Cape Heart Centre

Anzio Road

7925 Observatory, Cape Town, South Africa

Fax: +27-21-448 59 35

e-mail: peter.zilla@uct.ac.za

ABSTRACT

Objective

Constriction of vein grafts with braided external Nitinol meshes had previously led to the successful elimination of neo-intimal tissue formation. By knitting the meshes rather than braiding we investigated whether pulse compliance, smaller kink-free bending radius and milder medial atrophy can be achieved without losing the suppressive effect on intimal hyperplasia.

Methods

Pulse compliance, bending stiffness and bending radius as well as longitudinal-radial deformation-coupling and radial compression were compared in braided and knitted Nitinol meshes. Identical to previous studies with braided mesh-grafts, a senescent non-human primate model (Chacma baboons/ bilateral femoral interposition grafts/ 6 months) mimicking the clinical size-mismatch between vein grafts and run-off arteries was used to examine the effect of knitted external meshes on vein grafts (Nitinol mesh- constricted [group 1]; Nitinol mesh-constricted and fibrin sealant (FS) spray-coated for mesh attachment [group 2]; untreated control veins [group 3] and FS spray-coated control veins [group 4]).

Results

Compared to braided meshes knitted meshes had 3.8 times higher pulse compliance (3.43 ± 0.53 versus $0.94 \pm 0.12/100\text{mmHg}$; $p=.00002$); 30 times lower bending-stiffness (0.015 ± 0.002 versus $0.462 \pm 0.077 \text{ Nmm}^2$; $p=.0006$); 9.2 times narrower kink-free bending radius (15.3 ± 0.4 versus $140.8 \pm 22.4 \text{ mm}$; $p=.0006$) and 4.3 times lower radial narrowing caused by axial distension (18.0 ± 1.0 versus $77.0 \pm 3.7\%$; $p=.00001$). Compared to mesh-supported grafts, neointimal tissue was 8.5 times thicker in controls (group I: $195 \pm 45 \mu\text{m}$ vrs group III: $23.0 \pm 21.0 \mu\text{m}$; $p<.001$) corresponding with a 14.3-times larger neointimal area (group I: $4,330 \pm 957 \times 10^3 \mu\text{m}^2$ versus

group III: $303 \pm 221 \times 10^3 \mu\text{m}^2$; $p < .00004$). FS had no significant influence. Medial muscle mass remained at 43.4% in knitted meshes compared to 28.1% previously observed in braided meshes.

Conclusion:

Combining the suppression of intimal hyperplasia with a more physiological remodelling process of the media, manifold higher kink-resistance and lower fraying than in braided meshes makes knitted Nitinol an attractive concept in external vein graft protection.

INTRODUCTION

Attempts to improve vein graft performance through external mesh support go back several decades.¹⁻⁶ More recently, it emerged that a key-principle of mesh protection is diameter constriction.⁷⁻⁹ By reducing the size mismatch between vein grafts and run-off arteries, constriction leads to reduced circumferential stress and increased shear stress and thereby inhibits neo-intimal tissue formation.^{10, 11} Yet, external mesh support also introduces foreign materials and structures, both associated with peculiar biomechanics, biocompatibility and tissue responses. Non-pervious meshes, for instance, were shown to augment rather than mitigate intimal hyperplasia.⁵ Similarly, polymeric mesh materials are known to cause a strong foreign-body inflammatory response associated with the release of inflammatory cytokines that may induce intimal hyperplasia.¹² Alternatively, metals have been used for vascular stents for more than two decades and are known to elicit hardly any inflammatory response. Initial attempts to use loosely braided metal meshes for external vein support were already reported in the 1990s.¹³ Apart from mitigating neointimal tissue formation they were shown to protect the vein grafts against compression and deformation.¹⁴ Our own group used metal meshes to

demonstrate that, in order to achieve optimal suppression of diffuse intimal hyperplasia,⁷ the degree of overall constriction needs to aim at a diameter match of vein graft and host artery.⁸ Furthermore, by introducing the super-elastic shape memory alloy Nitinol as a mesh material, persistent longitudinal pleating of braided meshes became possible thereby allowing extreme constriction of vein grafts without the occurrence of wall folding. However, as much as braided Nitinol meshes were capable of proving the importance of graft constriction in the absence of an appreciable inflammatory response, they do not optimally address other crucial aspects of mesh support. One of these aspects is the need to eliminate diameter irregularities. By eradicating the eddy blood flow accompanying luminal irregularities, constriction to a constant diameter would not only address diffuse but also focal intimal hyperplasia.¹⁵ As braided meshes ‘snuggle’ against a vein wall like ‘Chinese finger catchers’, their capacity to maintain a constant diameter is limited. Moreover, it is almost inevitable to avoid longitudinal stretching of braided meshes during placement. As a consequence, additional unintended constriction ensues unless a spacer-rod or full-length balloon is inserted into the lumen¹⁶ – a measure that would lead to significant endothelial damage. Therefore, ideal meshes would have a structure that does not lead to unrestricted diameter narrowing when stretched.

Apart from the need for diameter-consistent meshes, it is biologically desirable to also integrate a certain degree of pulse compliance. The dramatic atrophy of the media seen in veins supported by non-compliant meshes⁶⁻⁸ confirmed previous observations that pulsed circumferential deformation is needed for maintaining a certain thickness of the media. As vascular smooth muscle cells have been shown to release factors with long-term physiological effects on endothelial cells (EC),^{17, 18} a functionally responsive and well-developed media is desirable. Since other issues such as fraying and bending-radius also contribute to the surgical performance of external vein meshes, a second generation of vein meshes needs to address a variety of structure-related aspects that go beyond the baseline-need of constriction.

Therefore, we assessed a Nitinol mesh structure with interlocking loops against the previously established braid. Once the physical test data suggested that the desired improvements to the mesh structure had been achieved, the knitted meshes were used for vein graft constriction in long-term primate implants.

MATERIALS AND METHODS

NITINOL MESHES

Based on previous diameter optimization in the same animal model^{7,8} and for comparative purposes an inner diameter (ID) of 3.39/3.37mm (at 120/80mm Hg) was chosen for the Nitinol meshes. Nitinol (BB Ni-Ti alloy: Nickel 56.0 wt%, Titanium 43.9365 wt%, Carbon 0.033 wt%, Oxygen 0.028 wt%, Hydrogen 0.0025 wt%) wires (thickness: 50 μ m; Fort Wayne Metals, Fort Wayne, IN, USA) were either braided using a 24-wire braiding machine (Medtronic Vascular, Danvers, USA) or knitted using a knitting machine with an 8-needle head (Lamb Inc, Chicopee, MA) (*Figure 1*). Replicates of n=3 and n=4 were used for the measurement of physical properties and for compliance testing, respectively.

Mesh Surface Area

The Nitinol surface area was calculated from the mass of the mesh per unit length, the material density of Nitinol (6.45 g/cm³) and the diameter of the Nitinol wires (n=3). The Nitinol surface area was related to the area of the abluminal surface of the vein inside the mesh at a 'resting' diastolic pressure of 80 mmHg. The adventitial surface area of the vein was calculated by assuming the outer diameter of the vein to coincide with the inner diameter of the mesh.

Pulse Compliance

Compliance was measured by volumetric displacement testing (DCT3 compliance tester, Dynatek Dalta, Galena, MS, USA). The mesh sample (n=4) was placed over a hyper-compliant silicon tube and inflated (distilled water, 37°C) and the internal pressure cycled at 70bpm between 80 mmHg and 120 mmHg. The change in water volume between the two pressure values was monitored and subsequently used to calculate radial compliance under compensation of the stiffening effect of the silicon tubing. Pulse compliance was expressed as percentage diameter-expansion between diastole (80mm Hg) and systole (120mm Hg).

Bending Stiffness and Radius

The bending stiffness was determined from a deflection test (air, room temperature) of mesh samples (n=3). A rod was inserted into mesh samples and the maximum deflection of a free length of mesh (20 mm for knitted, 40 mm for braided) due to the mesh's weight was measured with a ruler. The bending stiffness EI_y was calculated according to

$$EI_y = \frac{5ql^4}{384f_m}$$

where q is the weight per unit length, l is the sample length and f_m is the deflection.

The bending radius r_b of the braided mesh was calculated from the deflection test data using

$$r_b = \frac{l^2 + f_m^2}{2f_m}$$

whereas it was measured using a cone test for the knitted mesh. The two different methods were required due to the large difference in bending stiffness of the two mesh types rendering the cone test unsuitable for the braided mesh whereas the mathematical calculation could not be applied to the knitted mesh.

Longitudinal-Radial Deformation Coupling

The coupling of longitudinal and radial (i.e. transverse) deformation was assessed in uni-axial tensile testing (Instron 5544; Instron, Norwood, MA; air, room temperature) of mesh samples (n=3; sample length: 55 mm, gauge length: 40 mm). The samples were distended longitudinally until the tensile force rose sharply indicating an onset of locking. Longitudinal extension and force were recorded during the test. At 5% increments of longitudinal strain, macroscopic images (Canon D60, Canon, Tokyo, Japan) of the mesh were recorded to document the radial dimension of the mesh. The mesh diameter was measured in each macroscopic image using digital image analysis (Photoshop, Adobe Inc, San Jose, CA).

Radial Compression

The resistance against radial compression was determined in uni-axial compression test (Instron 5544; Instron, Norwood, MA; air, room temperature) of mesh samples (n=3; length: 40 mm). Samples were compressed radially to a maximum compression of 75%. Compression extension and force were recorded during the test. Samples were restrained longitudinally by fixing 5mm of the either end to the test head.

EXPERIMENTAL SURGERY

This study was approved by the Institutional Review Board of the University of Cape Town. Surgery and animal care complied with the Guide for the Care and Use of Laboratory Animals, Institute of Laboratory Animal Resources, Commission on Life Sciences, National Research Council. Washington: National Academy Press, 1996.

Adult Chacma baboons (n=12; 27.0±5.1kg) were provided by the breeding and quarantine facilities of the South African Medical Research Council (MRC) at Delft/Cape Town.

Superficial femoral veins were used as bilateral femoral artery interposition grafts (n_Σ=24 / n=6 per group / length 55.6±5.4mm) which were previously shown to resemble human saphenous vein grafts both with regards to size-mismatch and wall composition^{7,8}. One implantation in each subject was a control graft whereby the implantation side for the mesh grafts alternated between successive animals.. Vein harvest methods strictly followed no-touch principles to prevent spasm and thus allow for the assessment of in-situ dimensions. Meshes were applied by gently pulling the veins through an introduction straw on which the Nitinol mesh was mounted. At completion of the anastomoses (running 7/0 Prolene; Ethicon Inc., Somerville, New Jersey, USA) the mesh was briefly slipped back towards the middle of the graft and the cross-clamp was intermittently opened to allow the measurement of the OD of the distended vein graft without Nitinol mesh support. Two groups were additionally sprayed with

fibrin sealant (FS) [Tisseel®, Baxter International, Inc.] after the cross-clamp was removed to determine a possible biological effect of the attachment glue for the mesh. As such, four groups were compared: group I (mesh constriction without FS; n=6); group II (mesh constriction with FS; n=6); group III (controls without FS; n=6) and group IV (controls with FS; n=6). No anti-aggregatory medication was given post-operatively. All grafts were explanted after 180 days. At explantation grafts were perfusion-rinsed with heparinized Ringer's solution before perfusion fixation with 1L of 10% formalin in PBS (iliac cannulation; perfusion pressure of 120mm Hg). Given the natural recoil tendency of a non-pressurized artery, vessels were fixed at systolic pressures to preserve those luminal dimensions for analysis which exist during the forward flow phase. The grafts and the surrounding tissue were resected *en bloc*. After a 15mm long central specimen underwent macroscopic image analysis before it was further sub-divided and embedded in resin and processed for electron microscopy.

MORPHOLOGICAL ANALYSIS

Macroscopic vein graft analysis using image analyses of midgraft sections (QWinPro V 2.5; Leica Microsystems Imaging Solutions) was previously described in detail.^{7,8} Macroscopically obtained luminal dimensions were cross checked with microscopic measurements calculated on the basis of ODs, wall thicknesses of control samples, fixation-related shrinkage quotient and previously determined tissue compression within a mesh under arterial pressures.^{7,8}

Dimensional mismatch between vein grafts and host arteries was expressed as the quotient of cross sectional areas $Q_c = a_h/a_g$ whereby a_h represented the cross sectional area of the host artery and a_g that of the interposition graft with $Q_c = 1$ representing a perfect size match.

Resin Histology:

Wire-containing anastomotic- and mid-graft sections were infiltrated with methyl methacrylate resin (MMA) (Sigma-Aldrich, Steinheim, Germany). Dynamic sample-infiltration was done

over 3 days through increasing concentrations of benzoyl peroxide followed by cold curing polymerization for 72 hrs at -20°C under exclusion of air. Initially 100µm sections were cut with an *Isomet Precision Saw* (Buehler, Dusseldorf, Germany) and then ground down to between 4-8 µm with a *Metaserve 2000* (Buehler) grinder, using 2 grades (600 and 1200 grit) of paper to polish. The resin was not removed and the slides were stained with H&E before being mounted with *Glycergel* (Dako Cytomation, Glostrup, Denmark A/S), an aqueous mounting medium. Thin sections were cut on a Leica Polycut using a tungsten carbide blade and the resin removed with 2-methoxyethylacetate to enable staining with elastic masons and movat. Two series approximately 300µm apart were analysed. Specimens were viewed under a Nikon E 1000M and a Nikon Coolscope (Nikon, Tokyo).

Image Analysis:

Using Eclipse Net (Laboratory Imaging, Prague, Czech Republic) software composite images were assembled from digital single-frames that were captured at 4x or 10x magnification (Nikon Eclipse 90i and Nikon Coolscope). Lumen- and mesh-dimensions were obtained from resin sections. *Intimal hyperplasia tissue* (IH) was discernable by its demarcation through a largely present internal elastic lamella (IEL). *Muscularity* was defined as the partial cross sectional area of media smooth muscle cells within the boundaries of the media. After delineating the media between the internal elastic membrane and the adventitia, the measured actin-positive area was subtracted and expressed as a percentage of the total cross sectional area of the media

Scanning Electron Microscopy

After SEM preparation^{7,8} images were digitally captured by Orion V5.20 software (Orion, Brussels, Belgium) at 15x magnifications. Surface endothelialization was quantified using Scion

Image Software (NIH, Bethesda, USA). When the low-magnification pictures were inconclusive zooming-in on parallel live-images allowed verification.

Faxitron Analysis

The integrity of the Nitinol mesh at explantation was assessed by faxitron analysis (Faxitron MX20; Faxitron X-ray Corporation, IL) using a 35KV setting. A scoring system was applied for wire breakage whereby zero was intact; one represented isolated, single wire breakage and two extended damage areas.

STATISTICAL ANALYSIS

Post-hoc comparisons between continuous data sets (n=6) were performed using the Student's unpaired t-test. Endothelial confluency data, which were seen to have unequal variances, were compared using non-parametric Kruskal Wallis/Wilcoxon testing. Patency data were compared using Fisher's exact test. Two-tailed p values <.05 were regarded as demonstrating statistical significance.

RESULTS

BIOMECHANICAL MESH CHARACTERIZATION

Knitted meshes required less wire material per mesh length than braided ones. The Nitinol mass of knitted meshes was 19% less than that of its braided counterparts ($0.388 \pm 0.004 \text{g/m}$ versus $0.478 \pm 0.017 \text{g/m}$; $p=.0008$) and the mesh surface area was 19% less ($0.45 \pm 0.01 \text{ mm}^2$ per mm^2 versus $0.56 \pm 0.02 \text{ mm}^2$ per mm^2 ; $p=.0008$). The pulse compliance of knitted meshes was 3.8 times that of braided ones [$1.36 \pm 0.20\%$ ($3.43 \pm 0.53\%/100\text{mm Hg}$) versus $0.36 \pm 0.04\%$ ($0.94 \pm 0.12\%/100\text{mm Hg}$); $p=.00002$] while the bending stiffness was 30 times lower in knitted meshes ($0.015 \pm 0.002 \text{ Nmm}^2$ knitted versus $0.462 \pm 0.077 \text{ Nmm}^2$ braided; $p=.0006$). The kink-free bending radius was 9.2 times narrower in knitted meshes ($15.3 \pm 0.4 \text{mm}$ knitted versus $140.8 \pm 22.4 \text{mm}$ braided; $p=.0006$). When exposed to axial distension, knitted meshes reached their limit at a moderate length increase of $18.8 \pm 2.6\%$ compared to $60.3 \pm 2.5\%$ in braided ones ($p=.00004$). Similarly, the maximal radial contraction caused by axial distension was $18.0 \pm 1.0\%$ in knitted meshes as opposed to $77.0 \pm 3.7\%$ in braided ones ($p=.00001$) (*Figure 2*). This limitation of radial contraction in knitted meshes was less an issue of fundamentally different radial contraction behaviour than the consequence of the rapid locking of knitted meshes in response to axial strain (*Figure 2*). Radial compression tests indicated a nearly linear increase of the compression force with the compression displacement and radial compression stiffness of $0.778 \pm 0.215 \text{N/mm}$ for the braid mesh and $0.136 \pm 0.003 \text{N/mm}$ for the knitted mesh ($p=.007$) (*Figure 3*).

IN VIVO PERFORMANCE OF KNITTED MESHES

Graft Dimensions

Confirming the clinical relevance of the model, unstricted vein grafts had a 6.05 ± 2.35 times larger cross sectional luminal area than their target vessels ($Q_c = 0.24 \pm 0.10$ [group I]; $Q_c = 0.18 \pm 0.06$ [group II]; $Q_c = 0.20 \pm 0.07$ [group III]; and $Q_c = 0.18 \pm 0.06$ [group IV]) (Table I). External mesh constriction eliminated this size discrepancy (*Figure 4;5*). By narrowing the graft diameter (ID) to $39.6 \pm 4.9\%$ of its original size vein graft dimensions became even mildly smaller than those of the target arteries ($Q_c = 1.39 \pm 0.25$; $p = .0000002$ [group I] and $Q_c = 1.31 \pm 0.25$; $p = .0000007$ [group II]) (*Figure 4;5*). Although mesh constriction caused a $57.5 \pm 6.2\%$ redundancy in outer vein graft circumference none of the vein grafts showed signs of longitudinal folding at the time of explantation.

At 6 months, the untreated control group (group III) had undergone moderate graft dilatation reflected in a $25.0 \pm 13.6\%$ ($p > 0.1$ NS) increase in sub-intimal diameter (SID). This trend was not observed in the fibrin sealant-sprayed control group ($+ 0.4 \pm 17.3\%$; $p > .9$ NS). As graft dilatation had largely been counteracted by intimal hyperplasia, the ID of group III had remained unchanged (-0.6% ; $p > .09$ NS) while that of group IV had decreased by 26.1% ($p < .02$). In both mesh supported groups vein graft dilatation (SID group I: $+17.5 \pm 7.5\%$; $p < .00001$ / group II: $+22.3 \pm 4.4\%$; $p < .000003$) corresponded with mesh dilatation (group I $+15.1 \pm 5.4\%$ and group II $24.8 \pm 7.2\%$). In the absence of neointimal tissue these increases in SIDs translated into increases in actual inner diameters (IDs) (group I: $+15.0\%$; $p < .0000002$) / group II $+25.2\%$; $p < .006$). Correspondingly, cross sectional quotients remained largely unchanged in the control group (group III: $Q_c = 0.19 \pm 0.09$; $p > .3$ NS) but increased – albeit without statistical significance – in FS-sprayed controls (group IV: $Q_c = 0.30 \pm 0.14$; $p > .9$ NS) reflecting a continual size mismatch between vein grafts and their run-off artery. In the mesh-supported groups, dilatation offset the initial over-correction leading to almost size-matched

IDs of grafts and target vessels at the time of explantation (group I: $Q_c=1.09\pm 0.33$; $p>.3$ NS / group II: $Q_c=0.94\pm 0.37$; $p<.7$ NS).

Graft Pathology

In all four groups 4/6 grafts were patent at 180 days. There was no significant correlation between graft occlusion and individual animals as only one occluded graft in each group had an occluded contralateral corresponding graft. In the patent grafts, both control groups showed a thick, whitish vessel wall at the time of explantation (*Figure 6*). On a microscopic level, wall thickness of controls almost doubled (group III: +99.3%; $p<.0002$ and group IV: +82.5%; $p<.0006$). Although FS-sprayed controls were in average 30.8% thicker than untreated ones the difference was non-significant ($p>0.1$ NS).

Mesh-supported groups showed a thin vessel wall with the tissue between the blood surface and the mesh being so delicate that the mesh was visible from the blood side (*Figure 6*). Yet, an overall increase in wall thickness of 48.6% (group I; $p<.04$) and 43.7% (group II; $p>0.06$ NS) was observed histo-morphologically over the course of 6 months.

Endothelium

Although 38% of mesh-supported grafts showed an uninterruptedly confluent endothelium versus none in the control groups at explant, the overall difference in surface coverage ($91.0\pm 8.9\%$ versus 79.2 ± 15.9) was not significant ($p<.2$). None of the grafts showed less than 2/3 of their surface confluent endothelialized.

Midgraft Intimal Hyperplasia

Both control groups showed distinct neo-intimal hyperplasia (NIH) tissue (*Figure 7*) that was sometimes mildly eccentric. Mesh supported vein grafts had largely a monolayer of endothelium resting on a thin layer of loose acellular matrix ($<10\mu\text{m}$ in thickness) or a thin

neointima consisting of a few layers of α -actin positive cells. The latter seemed to be associated with areas of wire breakage.

Compared to mesh-supported grafts neointimal tissue was 8.5-times thicker in controls (group I: $23.0 \pm 21.0 \mu\text{m}$ vrs group III: $195 \pm 45 \mu\text{m}$ $p < .001$) corresponding with a 14.3-times larger neointimal area (group I: $303 \pm 221 \times 10^3 \mu\text{m}^2$ vrs group III: $4,330 \pm 957 \times 10^3 \mu\text{m}^2$; $p < .00004$) (*Figure 8*). FS-spraying had no significant effect on neointimal hyperplasia (controls: intimal thickness $\times 1.6$; $p > 0.2$ NS / intimal area $\times 1.3$; $p > 0.3$ NS/ mesh-supported: intimal thickness $\times 1.5$; $p > 0.4$ NS / intimal area $\times 1.6$; $p > 0.2$ NS).

Anastomotic Intimal Hyperplasia

Meaned over 2.5mm from the anastomosis, neointimal tissue was 1.6x thicker than in the mid-graft region in controls (NS) and 3.7x thicker in mesh supported grafts (NS). When measured directly at the anastomosis, it was 1.5x thicker in controls (NS) and 2.7x thicker in mesh supported grafts (NS). In both controls and mesh grafts FS-spraying had no significant effect. Yet, in absolute terms NIH was still manifold thicker in controls than in mesh grafts. This difference was more pronounced at the proximal anastomosis [5.3x without FS ($328 \pm 95 \mu\text{m}$ vrs $62 \pm 41 \mu\text{m}$; $p < .01$) and 8.0x with FS ($311 \pm 54 \mu\text{m}$ vrs $39 \pm 26 \mu\text{m}$; $p < .0004$)] than at the distal one [2.9x without FA ($457 \pm 302 \mu\text{m}$ vrs $35 \pm 13 \mu\text{m}$; NS) and 2.4x with FS ($296 \pm 230 \mu\text{m}$ vrs $31 \pm 15 \mu\text{m}$; NS)]

Media

The so called 'arterialization' of vein grafts over time was not accompanied by an increase in smooth muscle volume in the control grafts. As a moderate increase in media thickness (from $110.3 \pm 19.0 \mu\text{m}$ to $178.8 \pm 38.2 \mu\text{m}$, $p < .0005$) was coupled with a distinct drop in muscularity (from $60.1 \pm 13.9\%$ to $32.7 \pm 14.34\%$; $p < .003$) there was even a 17.2% decrease in muscle mass

observed (from $1678 \pm 633 \times 10^3 \mu\text{m}^3/\text{mm}$ to $1199 \pm 737 \times 10^3 \mu\text{m}^3/\text{mm}$; $p > .2$ NS). There were no significant differences between FS-treated and untreated controls. In mesh-supported vein grafts, media thickness decreased by 41.6% (from $77.6 \pm 40.7 \mu\text{m}$ to $45.3 \pm 25.6 \mu\text{m}$; $p > .06$ NS). As muscularity remained stable ($60.1 \pm 13.9\%$ versus $62.7 \pm 18.6\%$; $p > .9$) the overall muscle mass decreased by 56.6% from $1190 \pm 449 \times 10^3 \mu\text{m}^3/\text{mm}$ to $538 \pm 267 \times 10^3 \mu\text{m}^3/\text{mm}$ ($p < .004$). There was a trend towards more circular orientation of the relatively densely packed smooth muscle cells in the mesh supported groups (*Figure 9*). At the anastomoses media thickness was 2.8x higher in controls (NS) and 3.5x in mesh grafts (NS) with no influence of FS or distal or proximal location.

Adventitia

Mesh support led to a dramatic reduction in adventitial thickness [-55.3% ($p < .006$) without FS and -40.1% ($p < .005$) with FS] (*Figure 7*). The effect of fibrin sealant was insignificant with regards to adventitial thickness [+ 11.2% (NS) in controls and +68.7% (NS) in mesh supported veins]. Yet, the outer capsule appeared thicker and the overall collagen content higher in the FS treated groups.

Faxitron Assessment of Mesh Integrity

None of the occluded grafts showed any signs of wire breakage. In the patent grafts, 63% of meshes showed local signs of wire breakages at the narrow loops of the knit in proximity to the proximal anastomosis near the hip joint (*Figure 10*). Half of the affected meshes showed the breakage to be limited to a few adjacent wires along one longitudinal row of loops while the other half showed similar lines of adjacent wire breakages in two or maximally three neighbouring rows of wire loops (*Figure 10*). None of the meshes showed multiple sites of wire breakage.

DISCUSSION

An external Nitinol mesh for vein grafts was developed that introduced the concept of stretch-resistant diameter-constancy, pulse-compliance and fraying resistance. Using an identical animal model and the same mesh diameter as in previous studies we could show that a knitted structure significantly improved the handling characteristics and biomechanics of braided meshes without reducing their dramatic effect on the suppression of intimal hyperplasia.

Given the similarity in vascular patho-biology between large, senescent chacma baboons and man,^{17, 18} this low-throughput animal model was chosen. As it represents a non-human primate model, a conscientious effort was made to keep the number of control groups to a minimum.

Overall, the advantages of a knitted mesh structure reached from better kink-protection to a more physiological remodelling of the vein grafts. From the surgical standpoint, the markedly lower bending stiffness and kink-free bending radius of knitted meshes can be expected to promote higher vein graft flexibility than braided meshes, thereby allowing an easier adaptation of the graft to anatomical requirements. As the kink-free bending radius was more than 9 times narrower than that of braided meshes, the anticipated effect is significant. Since the vein is abluminally glued to the mesh, the kink-free radius and the difference thereof between the two mesh types is expected to remain similar. This is also supported by the fact that the mechanical contribution of the pressurized vein inside the mesh is the same for knitted and braided mesh. Moreover, despite the low bending stiffness, knitted meshes exhibited a higher resistance against longitudinal stretching and the associated radial narrowing than braided ones. While the radial constriction resulting from longitudinal stretching was initially even higher in the knitted ($y = 0.0174 x^2 + 0.94 x$; $R^2=0.9995$) than the braided meshes ($y =$

$0.0136x^2 + 0.42x$; $R^2=0.9965$), longitudinal stretch and radial contraction were arrested as early as at 19% and 18%, respectively. In contrast, braided meshes permitted longitudinal stretching of 60% resulting in radial narrowing by as much as 77%. As a consequence of the arrest of longitudinal and radial deformation, knitted meshes can be expected to provide superior length- and diameter-stability for vein grafts, both during the implant procedure and thereafter. This becomes important when considering that physiologically, axial forces induced by transmural pressure reach 0.6 N at a moderate systolic pressure of 100 mmHg.¹⁹ At one third of these axial forces (0.2N) braided meshes already underwent an almost maximum longitudinal stretch associated with a three-quarter diameter constriction while knitted meshes stretched by a mere 11% and approached their deformation arrest at a force of 0.6N. Since the vein graft is fixed at both ends when implanted, the effects of early deformation arrest in the knitted mesh is expected to play a role in prevention of localised deformation in sections of the graft rather than over the entire graft length. In addition to the axial forces based on blood pressure, localised deformations, such as radial bulging, may also be induced by irregularities of the vein diameter where the limited deformation of the knitted meshes promotes a more even smoothing of the vein graft. To reduce the impact of this ‘Chinese finger catcher’ effect of braided meshes, full-length balloons were inserted in initial clinical studies to avoid graft constriction.¹⁶ However, apart from added complexity, the associated endothelial damage would not be compatible with contemporary ‘no-touch’ approaches to vein harvesting.²⁰ Moreover, even the lower compression-stiffness of knitted meshes may not be a disadvantage as the higher resistance of the braid is an integral part of the generally stiffer and less flexible nature of this mesh.

This stiffness is also reflected in the practically absent recoil compliance of braided meshes in spite of the use of a super-elastic material such as Nitinol. The term compliance needs to be defined as it is often used for outward expansion rather than full hysteresis. The pulsatile recoil

compliance of an artery between the systolic and the diastolic pressure is approximately 11.5%/100mmHg.²¹ As a vein graft reaches full outward distension at 30mm Hg which is below diastolic pressures, there will be no 'pulsatile' compliance in the arterial circulation without an external support that actively pushes the vein wall back during diastole. Although the pulse-compliance of knitted Nitinol meshes is less than half of that of an artery, it clearly generates diastolic reverse-force under physiological pressures and as such pulsatility. The media of blood vessels is a sensor organ for the biomechanical forces during cardiac cycles. In capacity vessels such as veins that hold 85% of the circulating blood volume without being exposed to pulse pressures, a collagen-rich media with a 45 degrees smooth muscle cell orientation provides an optimal adjustment tool for volume changes. In arteries, where resistance and pulse absorption are in the foreground, a muscle cell-rich, circularly oriented media best addresses these needs. Conventional vein grafts are adventitially locked in full distension and as such, their media does not encounter pulsatility. The result – often wrongly termed 'arterialization' – is in fact a distinct atrophy of smooth muscle cells accompanied by the doubling of intercellular collagen.^{7, 8, 22} Given the physiological importance of an arterial media both with regards to its interaction with the intima and its biomechanical shock-absorber function, one additional goal of mesh protection should therefore be a 'true arterialization' of the media of vein grafts. When vein grafts were constricted by tight, braided meshes, the degree of smooth muscle cell atrophy was even more pronounced than in control veins but in the absence of collagen it resulted in a densely compacted media of approximately one quarter of its previous thickness.⁸ Using the identical animal model in the current study, knitted meshes led to a distinctly milder degree of atrophy with almost 2/3 of the media thickness preserved. In the absence of sizable amounts of collagen in the compacted media, smooth muscle cells showed a preferentially circular alignment approximating the media orientation of arteries.

Further to kink-resistance and pulse-compliance, another advantage of a knitted structure is its fray-resistance. Previous clinical trials showed support-failures at the anastomosis of mesh grafts due to the proneness of braids towards fraying.¹⁶

As different wire densities are inherent to braids and knits, one could argue that the observed differences between the two structures merely reflect different void dimensions. The fact that the biomechanics of braided meshes remained relatively constant even when the wire density varied by a factor two,⁷ indicates that the distinctly different characteristics of knitted meshes are inherent to the structure rather than the wire density. However, although the braided mesh used had the lowest wire density reported, it still contained significantly more Nitinol per length than the knitted one. Even though Nitinol represents a particularly 'biocompatible' material compared to polymers, it nevertheless represents foreign matter and as such, providing superior biomechanical support with less material is clearly desirable. As the flimsy support mesh snugles loosely against the vein wall, attachment prior to the pressure filling of the graft is crucial during surgery. Given the wide use of FDA approved fibrin sealant in surgery and its successful application in previous studies with braided meshes^{7, 8, 16} a study that potentially represents a base line investigation into a new device needed to exclude the possibility of fibrin sealant having an effect on its own. Our results confirmed our preceding observation that more pronounced periadventitial fibrosis resulted in a trend towards diameter shrinkage of FS sprayed controls, without influencing the behavior of mesh grafts or the wall remodeling of any group.

While the biomechanical characteristics of knitted and braided meshes differed significantly, a basic underlying principle of mesh protection – namely the elimination of the diameter mismatch between vein grafts and run off arteries – applied regardless. Conservatively emulating clinical conditions of e.g. coronary artery bypass grafts where the Q_c is < 0.30 ,⁷ non

mesh-constricted control grafts in our study had a Q_c of < 0.25 and as such a four to five times higher cross sectional area than the target artery. Given the fact that shear stress declines non-linearly with the power of three of the vessel diameter, such a distinct caliber mismatch results in a dramatic decrease in shear stress in the over-dimensioned vein graft. As diffuse intimal hyperplasia (IH) is triggered by low shear stress and high wall stress, it follows from Pouseille's law that constrictive mesh sizes should counter neointimal proliferation. The estimated threshold for IH is a shear stress of 5 dynes/cm^2 .²³ In our previous studies IH was almost completely suppressed if the Q_c was > 0.45 ,⁷ a cross sectional vessel-to-graft ratio at which this threshold value for shear stress was exceeded. In our present study and its preceding twin-study where we used a braided mesh,⁸ the Q_c was > 1.3 and > 1.4 , respectively. Inasmuch as the deliberate narrowing of an existing vessel triggers a surgeon's apprehension, a small conduit diameter is fundamentally different from luminal narrowing due to pathological processes. No bypass conduit other than the internal thoracic artery, for instance, has a 10 year patency of more than 90%. Yet, its inner diameter is as small as 2.5mm ⁷ and its intima free of myo-fibrous proliferation. In contrast, saphenous vein grafts used for both coronary and infrainguinal bypasses show diffuse intimal hyperplasia in the initial 6-18 months followed by focal intimal hyperplasia that eventually lead to occlusive luminal narrowing in a significant proportion of grafts. The triggers for focal intimal hyperplasia are thought to be turbulences as a consequence of diameter irregularities. As such, while the short to medium term goal of mesh constriction is to increase shear forces to protective levels, the medium to long term goal is the elimination of luminal irregularities. We have previously shown that a diameter constriction of 27% on average would eliminate diameter irregularities in 98% of human saphenous vein grafts.²⁴ Naturally, there are limits to vein constriction as folding of the vein wall may be seen as detrimental. Yet, when analyzing 100 consecutive patients undergoing coronary artery bypass operations the use of four mesh sizes ranging from 3mm and 4.2mm would have

resulted in uninterrupted mesh support throughout and only 26% of total vein length being at risk of relatively mild wall folding.

After 6 months, a mesh dilatation of 9% was observed in the braided meshes⁷ and 15-24% in the knitted meshes. The more pronounced dilatation in the knitted meshes may have been partly attributable to a modest degree of wire breakage. The predominant location of broken wires in the patent grafts was in the proximal half that was affected when the leg was bent in the hip. At the same time, none of the occluded grafts showed any wire breakage. This suggests that breakages occurred at a late stage of implantation with external motion and prolonged pulse-strain jointly accounting for the fractures. At that stage the pulsatile effect of the mesh's recoil compliance may have been in place sufficiently long for 'training' the muscularity of the vessel wall. Therefore, in spite of the higher degree of mesh dilatation the thicker, more muscular vessel wall in knitted meshes resulted in a Q_c at 6 months of 0.97 as opposed to 0.91 in braided meshes.⁸ Both meshes still provided sufficient constriction for the vein grafts to remain safely within a shear stress range that suppressed IH. With no significant influence of fibrin sealant used for the attachment of the meshes to the vein wall, neointimal thickness was nine times less in mesh supported grafts and neointimal area was even 20 times less. The fact that in areas of wire breakage a neointima was sometimes mildly present in the form of a few layers of smooth muscle cells, highlights the role circumferential wall stress plays on top of shear stress. Notwithstanding the rather negligible effect of wire fractures, it is likely that alternative knitting patterns would prevent breakages without losing pulse compliance. Breakages were limited to the site where wires were bent at an acute angle as a result of the uneven knitting pattern where large loops alternated with narrow ones. Even knitting patterns would eliminate these sites of particularly high-stress. However, while even knits would most likely minimize wire breakage, they would not overcome the challenges imposed by knitting on the task of inserting the vein into the mesh without traumatizing

the vein. As much as diameter stability in response to axial mesh compression or stretching is an advantage of knitted meshes, it also deprives them of one advantage of braided meshes namely the ability of easily feeding the vein graft into an initially larger mesh diameter - a limitation that may well affect the use of the mesh for long peripheral bypass grafts. Whether this challenge may eventually be overcome by insertion-straws or micro-welded longitudinal slits that snap-close after insertion of the vein graft remains to be seen. For the time being, the more demanding insertion of the vein grafts into the knitted meshes may well have been the reason for the lower degree of surface endothelialization seen in the present study as compared to its preceding twin study using braided meshes. The absence of wire breakage in the occluded grafts suggesting early occlusions supports this presumption.

Nevertheless, the combined benefit of a near-total suppression of intimal hyperplasia with a more physiological remodelling response of the media, manifold higher kink resistance and for the most part the elimination of anastomotic fraying make knitted Nitinol meshes a highly attractive concept that holds a high incentive to overcoming remaining obstacles.

ACKNOWLEDGEMENTS

The study was mainly funded through a research collaboration grant by Medtronic Inc. (Minneapolis MN) to the University of Cape Town. It was partly funded by a THRIP grant of the National Research Foundation (South Africa) as well as a grant by the South African Medical Research Council (MRC) to the 'Cape Heart Group'. The authors wish to thank Adcock Ingram Critical Care for the generous donation of the Baxter Tisseel® fibrin kits used in this study.

REFERENCES

1. Parsonnet V, Lari AA, Shah IH. New Stent for Support of Veins in Arterial Grafts. *Arch Surg.* 1963;87:696-702.
2. Mehta D, George S, Jeremy J, Izzat M, Southgate K, Bryan A, et al. External stenting reduces long-term medial and neointimal thickening and platelet derived growth factor expression in a pig model of arteriovenous bypass grafting. *Nat Med.* 1998;4(2):235-9.
3. Barra J, Volant A, Leroy J, Braesco J, Airiau J, Boschat J, et al. Constrictive perivenous mesh prosthesis for preservation of vein integrity. Experimental results and application for coronary bypass grafting. *J Thorac Cardiovasc Surg.* 1986;92(3 Pt 1):330-6.
4. Kohler T, Kirkman T, Clowes A. The effect of rigid external support on vein graft adaptation to the arterial circulation. *J Vasc Surg.* 1989;9(2):277-85.
5. Violaris A, Newby A, Angelini G. Effects of external stenting on wall thickening in arteriovenous bypass grafts. *Ann Thorac Surg.* 1993;55(3):667-71.
6. Vijayan V, Shukla N, Johnson J, Gadsdon P, Angelini G, Smith F, et al. Long-term reduction of medial and intimal thickening in porcine saphenous vein grafts with a polyglactin biodegradable external sheath. *J Vasc Surg.* 2004;40(5):1011-9.
7. Zilla P, Human P, Wolf M, Lichtenberg W, Rafiee N, Bezuidenhout D, et al. Constrictive external nitinol meshes inhibit vein graft intimal hyperplasia in nonhuman primates. *J Thorac Cardiovasc Surg.* 2008;136(3):717-25.

8. Zilla P, Wolf M, Rafiee N, Moodley L, Bezuidenhout D, Black M, et al. Utilization of shape memory in external vein-graft meshes allows extreme diameter constriction for suppressing intimal hyperplasia: a non-human primate study. *J Vasc Surg.* 2009;49(6):1532-42.
9. Franz T, Human P, Dobner S, Reddy BD, Black M, Ilsley H, et al. Tailored sizes of constrictive external vein meshes for coronary artery bypass surgery. *Biomaterials.* 2010;31(35):9301-9.
10. Morinaga K, Okadome K, Kuroki M, Miyazaki T, Muto Y, Inokuchi K. Effect of wall shear stress on intimal thickening of arterially transplanted autogenous veins in dogs. *J Vasc Surg.* 1985;2(3):430-3.
11. Koo E, Gotlieb A. Neointimal formation in the porcine aortic organ culture. I. Cellular dynamics over 1 month. *Lab Invest.* 1991;64(6):743-53.
12. Shimokawa H, Ito A, Fukumoto Y, Kadokami T, Nakaike R, Sakata M, et al. Chronic treatment with interleukin-1 beta induces coronary intimal lesions and vasospastic responses in pigs in vivo. The role of platelet-derived growth factor. *J Clin Invest.* 1996;97(3):769-76.
13. Zurbrugg HR, Zirngibl H. [Improvement of venous diameter in bypass surgery: initial applications of ultraflexible biocompound grafts in patients]. *Swiss Surg Suppl.* 1996;Suppl 1:8-12.
14. Krejca M, Skarysz J, Szmagala P, Plewka D, Nowaczyk G, Plewka A, et al. A new outside stent--does it prevent vein graft intimal proliferation? *Eur J Cardiothorac Surg.* 2002;22(6):898-903.

15. Liu S. Prevention of focal intimal hyperplasia in rat vein grafts by using a tissue engineering approach. *Atherosclerosis*. 1998;140(2):365-77.
16. Zurbrugg H, Knollmann F, Musci M, Wied M, Bauer M, Chavez T, et al. The biocompound method in coronary artery bypass operations: surgical technique and 3-year patency. *Ann Thorac Surg*. 2000;70(5):1536-40.
17. Zilla P, Bezuidenhout D, Human P. Prosthetic vascular grafts: Wrong models, wrong questions and no healing. *Biomaterials*. 2007;28(34):5009-27.
18. Zilla P, Preiss P, Groscurth P, Rosemeier F, Deutsch M, Odell J, et al. In vitro-lined endothelium: initial integrity and ultrastructural events. *Surgery*. 1994;116(3):524-34.
19. van Andel CJ, Pistecky PV, Borst C. Mechanical properties of porcine and human arteries: implications for coronary anastomotic connectors. *Ann Thorac Surg*. 2003;76(1):58-64.
20. Souza DS, Johansson B, Bojo L, Karlsson R, Geijer H, Filbey D, et al. Harvesting the saphenous vein with surrounding tissue for CABG provides long-term graft patency comparable to the left internal thoracic artery: results of a randomized longitudinal trial. *J Thorac Cardiovasc Surg*. 2006;132(2):373-8.
21. Konig G, McAllister TN, Dusserre N, Garrido SA, Iyican C, Marini A, et al. Mechanical properties of completely autologous human tissue engineered blood vessels compared to human saphenous vein and mammary artery. *Biomaterials*. 2009;30(8):1542-50.
22. Szilagyi D, Elliott J, Hageman J, Smith R, Dall oC. Biologic fate of autogenous vein implants as arterial substitutes: clinical, angiographic and histopathologic observations in femoro-popliteal operations for atherosclerosis. *Ann Surg*. 1973;178(3):232-46.

23. Sho E, Nanjo H, Sho M, Kobayashi M, Komatsu M, Kawamura K, et al. Arterial enlargement, tortuosity, and intimal thickening in response to sequential exposure to high and low wall shear stress. *J Vasc Surg.* 2004;39(3):601-12.

24. Human P, Franz T, Scherman J, Moodley L, Zilla P. Dimensional analysis of human saphenous vein grafts: Implications for external mesh support. *J Thorac Cardiovasc Surg.* 2009;137(5):1101-8.

Table 1: Dimensional relations of vein grafts and run-off arteries before and after mesh support as well as before and after 24 weeks of implantation. The femoral Chacma baboon model provides a cross sectional quotient (Q_c) of 0.18 to 0.24 without mesh support, moderately exaggerating the size mismatch seen between vein grafts and target arteries in clinical coronary artery bypass grafting. Taking a degree of mesh expansion into account, the inner diameter (ID) of mesh-supported grafts perfectly matches that of the run-off artery at the time of explantation.

		Sup. Fem. A. (SFA)		Superficial Femoral Vein (SFV)				Q_c SFV _D / SFA (without mesh / at implant)	SF Vein Graft		Q_c SFV _G / SFA (with mesh / at implant)	SF Vein Graft	
		In Situ		In Situ		Distended			At Implant			At Explant (24w)	
		ID	OD	ID	OD	ID	OD		ID	OD		ID	Patency
Gr I	Mesh	3.26±0.45	4.07±0.43	5.81±0.94	7.00±1.36	6.86±1.03	7.82±1.07	0.24±0.10	2.83±0.03	3.68±0.00	1.39±0.29	3.25±0.10	4/6
Gr II	Mesh+FG	3.27±0.41	4.17±0.24	7.00±1.10	7.82±1.19	7.99±1.41	8.90±1.41	0.18±0.06	2.86±0.13	3.77±0.00	1.31±0.25	3.59±0.46	5/6
Gr III	Control	3.09±0.43	3.97±0.33	6.35±1.02	7.22±0.99	7.20±1.05	8.07±1.01	0.20±0.07	7.20±1.05	8.01±1.01	0.20±0.07	7.16±0.50	4/6
Gr IV	Control+FG	3.02±0.43	3.88±0.40	5.89±1.29	6.88±1.30	7.39±1.11	8.38±1.14	0.18±0.06	7.39±1.11	8.38±1.14	0.18±0.06	5.46±1.01	4/6

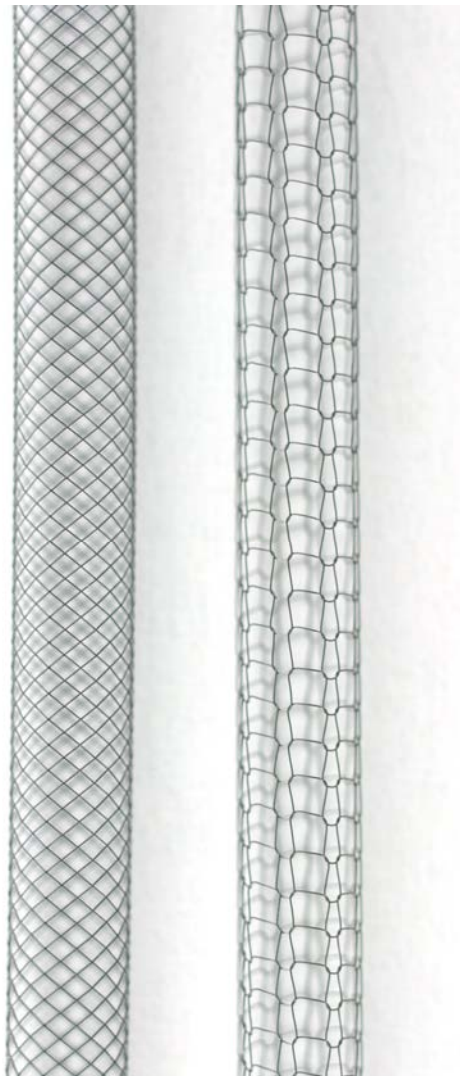
FIGURES

Figure 1: Macro-photograph comparing a braided mesh (left) with a knitted one (right). The knitting pattern is uneven with large loops alternating with narrow ones.

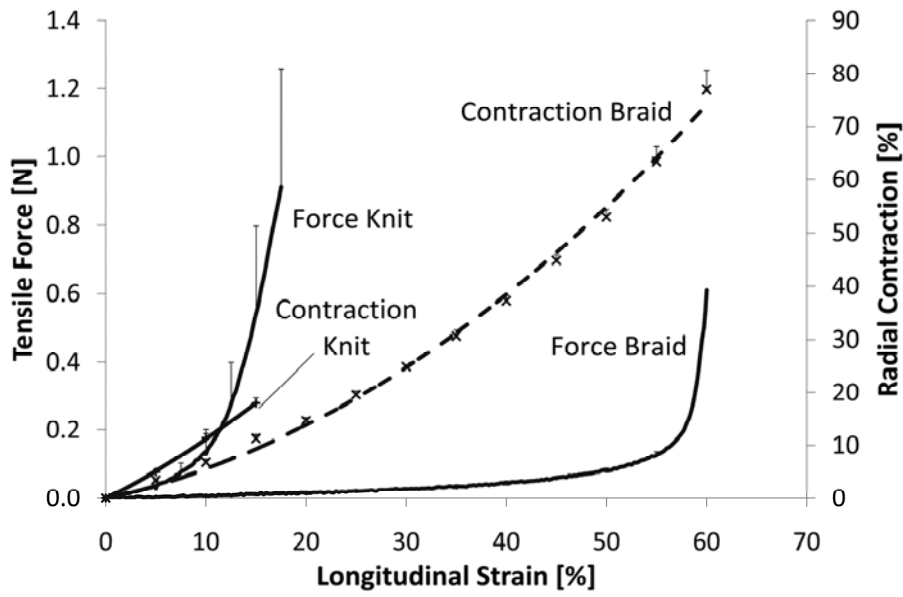


Figure 2: Tensile force and radial contraction (narrowing) versus longitudinal strain (stretch) of the braided and knitted mesh samples.

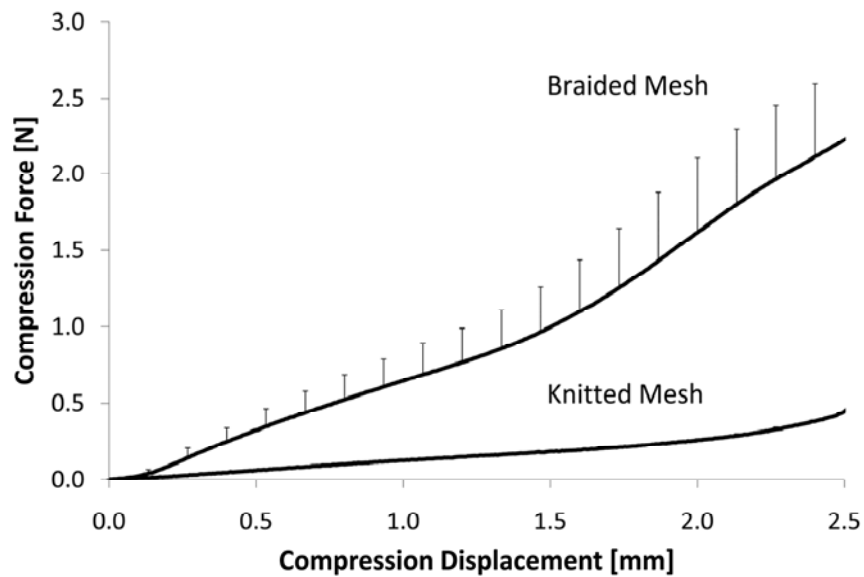


Figure 3: Compression force versus compression-displacement for braided and knitted meshes.

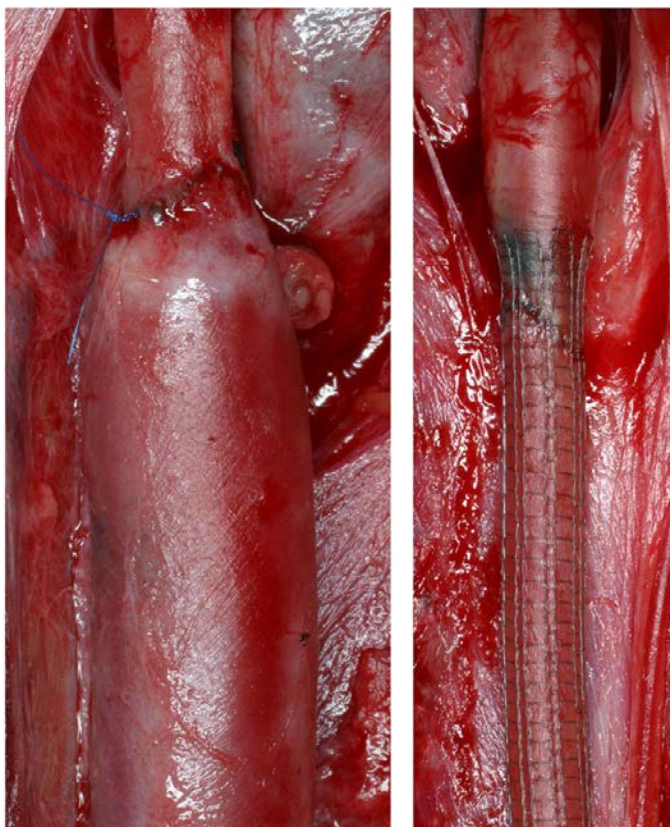


Figure 4: Anastomotic region of a control graft and a mesh-supported vein graft at implantation. While the control graft shows the typical size mismatch the femoral model provides between vein graft and target artery, the mesh-graft shows that a vein constriction was chosen that reduced the graft diameter even mildly below that of the artery. One can clearly see that the contractility of the vein allows such a distinct diameter constriction without wall folding.

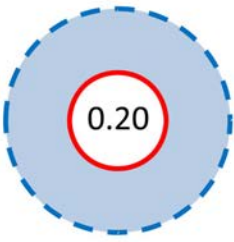
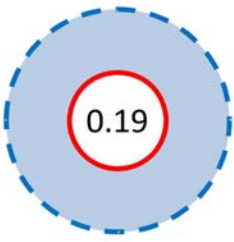
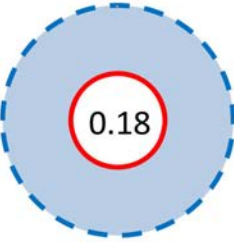
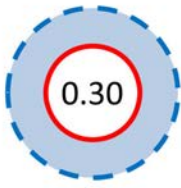
IMPLANT	EXPLANT
	
Control	
	
Control + FS	
	
Mesh	
	
Mesh + FS	

Figure 5: Graphical illustration of cross sectional discrepancies between vein grafts and their target artery at the time of implantation and at explant. While the target arteries are represented by the red circles, the vein grafts are shown as blue interrupted lines. In the control group the only mildly increased cross sectional quotients (Q_c from 0.20 to 0.18) betrays the degree of intimal hyperplasia as a 25% subintimal dilatation was compensated by neointimal tissue. In fibrin sealant-sprayed controls, the typically stronger wall fibrosis led to a 26.1% decrease in subintimal diameter, exaggerated by distinct neointimal proliferation (Q_c from 0.16 to 0.30). In both mesh groups, an almost perfect size-match was obtained after 6 months of implantation resulting from mild dilatation of the initially slightly over-constricted meshes.



Figure 6: Macroscopic appearance of vein grafts after 6 months of implantation. While control grafts showed a thickened, whitish vessel wall and a distinctly larger diameter, mesh-supported grafts had a delicate, translucent wall with the mesh visible throughout.

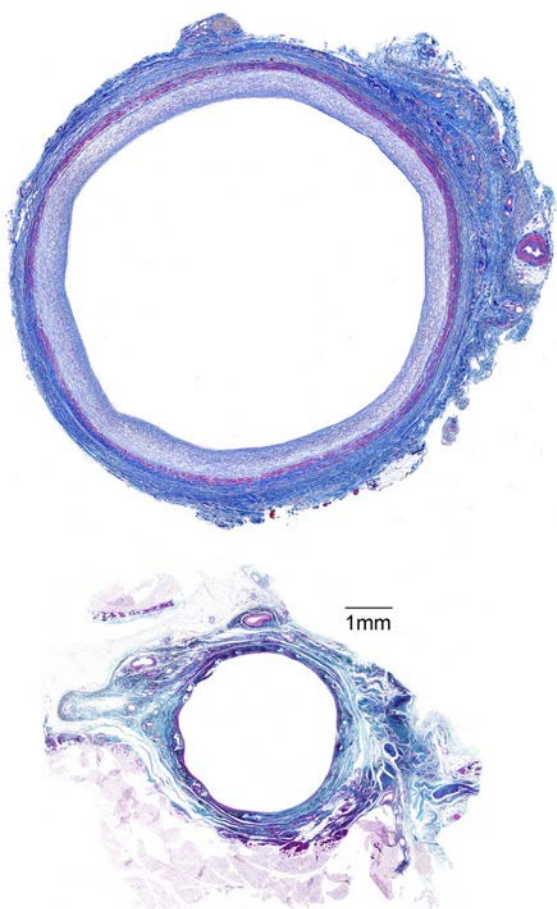


Figure 7: Histological cross sections of mid-grafts at identical magnification (stitched at x40; Azan stain) showing the marked diameter difference between controls (top) and mesh-supported (bottom) grafts. The methacrylate-embedded, tungsten-cut section of the mesh-graft shows the Nitinol wires, demarcating the delicate vessel wall from the surrounding tissue. A distinct layer of diffuse neointimal tissue narrows the lumen of the control grafts by almost a millimetre (see length bar).

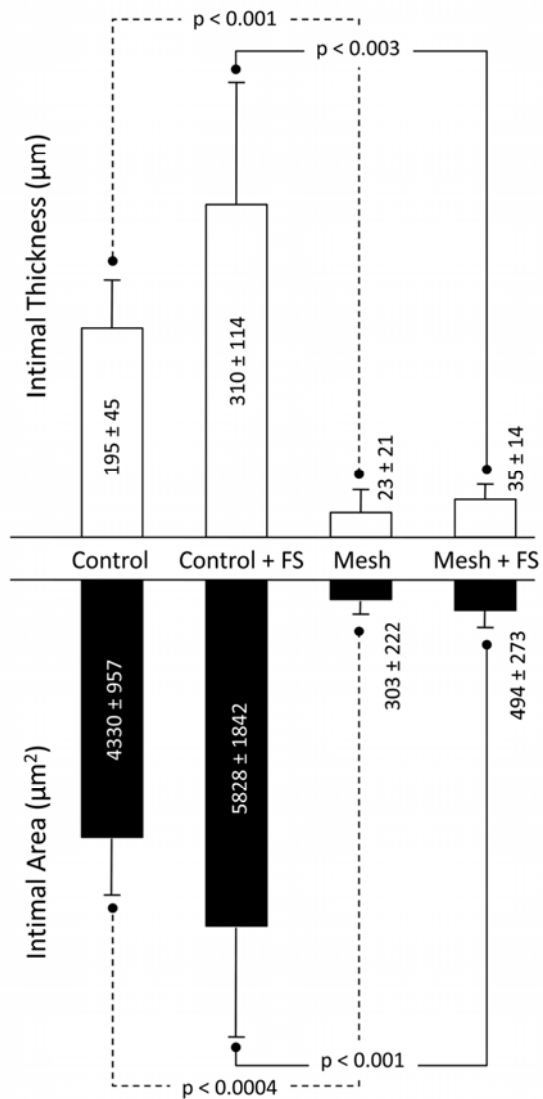


Figure 8: Comparison of intimal thickness (top) and intimal area (bottom) between the groups.

Non mesh-supported controls showed an 8.5 times higher intimal thickness and 14.3 times higher intimal area than mesh-grafts. In both groups spraying with fibrin sealant (as a means to firmly attach the mesh to the vein wall) had led to more pronounced neointimal proliferation.

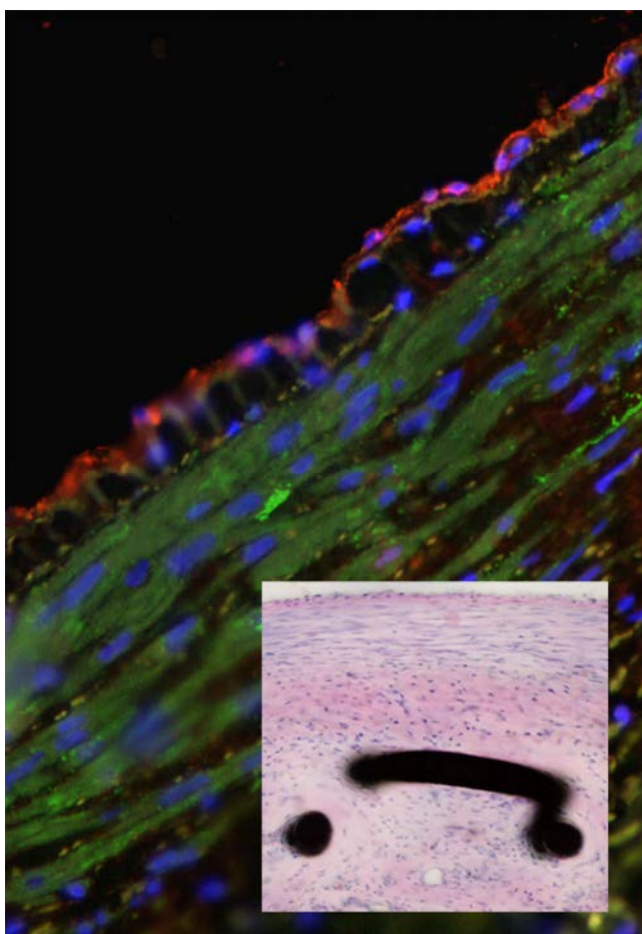


Figure 9: Double-stain (CD31/ α -Actin/ Dapi) of methacrylate-embedded and tungsten-cut mesh-graft. A monolayer of CD 31-positive endothelial cells lies loosely on the autofluorescing, yellow internal elastic lamella that separates it from the media. The strongly α -Actin-positive media consists of densely compacted smooth muscle cells with elastin fibres interspersed. The longitudinal orientation of the Dapi-positive nuclei underlines the circumferential orientation of the smooth muscle cells of the cross section. The insert shows a well preserved wire-loop of the Nitinol mesh on a saw-grounded section. Although the H.E. stains of such sections do not allow the colour-distinction between structures, one can still recognize the thin intima, the well-developed, aligned media and the pinker, collagen-rich adventitia underneath the Nitinol struts as opposed to the looser outside tissue.

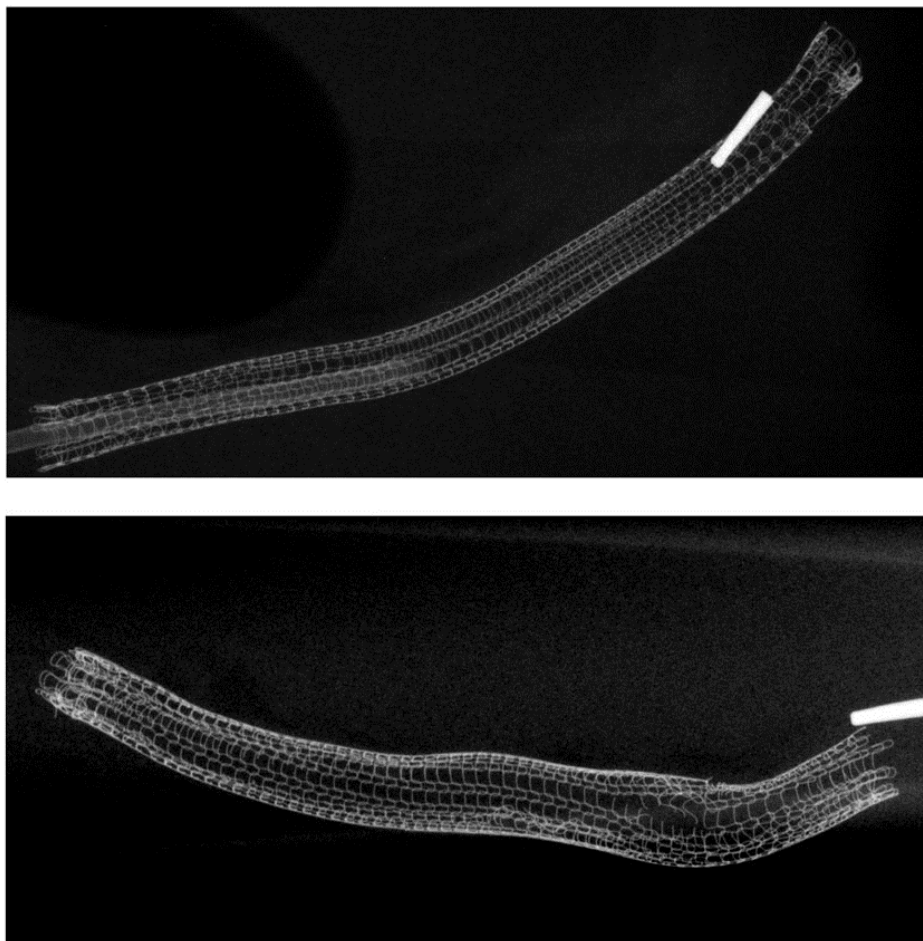


Figure 10: Faxitron picture of an occluded graft (top) and a patent one (bottom). The clip indicates the proximal side. In the patent graft, wire breakages are visible in the proximal third, closer to the area affected by hip bending. Breakages are exclusively found at the interlocking angles of the wire loops of the knitted mesh structure. The fact that breakages are absent in all occluded grafts indicates that graft occlusions occur early and that hemodynamic strain also contributes to the tiring of struts.